Available online at www.sciencedirect.com

SciVerse ScienceDirect

journal homepage: www.elsevier.com/locate/issn/15375110

Research Paper

A monocular vision-based diameter sensor for *Miscanthus giganteus*

*Lei Zhang, Tony E. Grift**

Department of Agricultural and Biological Engineering, University of Illinois, 1304 W. Pennsylvania Avenue, Urbana, IL 61801, USA

ARTICLE INFO

Article history:
Received 3 September 2011
Received in revised form
4 December 2011
Accepted 28 December 2011
Published online 21 January 2012

The stem diameter of *Miscanthus giganteus* (MxG) is an important parameter in the measurement of stand volume and yield. To measure the diameters of MxG stems automatically, a vision-based diameter sensor was developed, consisting of a camera and a laser sheet that was slanted downward at a 15° angle. The laser sheet projected Illuminated Line Segments (ILSs) onto the MxG stems, creating detectable features in images that enabled the depth from the camera to the stems and, subsequently, the stem diameters to be measured.

To evaluate the method in a sample of 1364 MxG stems, originating from 100 randomly selected images, the depths and diameters of 150 stems were measured manually and plotted versus their automatically measured counterparts. Straight lines with intercept were fitted to both the depth and diameter data. The depth measurements, ranging from 368 to 1486 mm, yielded a slope of 1.002, an intercept of −1.2 mm and a coefficient of determination of 0.998. The diameter data, ranging from 3.1 to 14.6 mm, yielded a slope of 0.845, an intercept of 1.4 mm and a coefficient of determination of 0.926.

1. Introduction

Bioenergy is becoming one of the main energy resources of global sustainable development (Yamamoto, Yamaji, & Fujino, 1999). It is also considered as a solution to the problems of global warming and environment damage from fossil fuels (Michel et al., 2011). Owing to its ability to adapt to different soils and climates, low nutrition requirement and high yield, *Miscanthus giganteus* (MxG) is considered one of the major energy crops worldwide (Clifton-Brown, Breuer, & Jones, 2007; Lewandowski, Scurlock, Lindvall, & Christou, 2003; Michel et al., 2011). Its dry matter yield can achieve 33 t ha in Illinois (Heaton, Clifton-Brown, Voigt, Jones, & Long, 2004). The stem diameter of MxG is one of the yield-related morphological parameters (Zub, Arnoult, & Brancourt-Hulmel, 2011), as well as an indicator of its genotype (Clifton-Brown & Lewandowski, 2002). To date, the MxG stem diameter is typically measured manually using callipers, a tedious and error-prone practice.

The activity of diameter sensing is ubiquitous in agriculture, forestry and orchards. Delwiche and Vorhees (2003) developed a diameter sensor for deciduous trees, using an infrared laser optoelectronic system where the reported accuracy of the sensor was ±1.9 mm. An optical time-of-flight based diameter sensor for mature trees with a reported accuracy of 10 mm was developed by McDonald, Rummer, and Grift (2003). The time-of-flight principle was also used to develop a root collar diameter sensor for pine seedlings (Grift & Oberti, 2006). This sensor achieved an accuracy of 0.1 mm–0.3 mm depending on conditions and configurations. Unfortunately, the diameter measurement principles as reported are not suitable for application in an MxG field, since

* *Corresponding author.*
E-mail addresses: grift@illinois.edu, grift@uiuc.edu (T.E. Grift).
1537-5110/$ – see front matter © 2011 IAgrE. Published by Elsevier Ltd. All rights reserved.
doi:10.1016/j.biosystemseng.2011.12.007

Notation

α	Downward slope of the laser sheet in, ° (constant)
β	Camera parameter, ° (constant)
C	Intercept between upper field of view of the camera and the laser sheet, mm (constant, Figs. 2 and 4)
D	Distance ("Depth") between the camera pinhole and a *Miscanthus* stem, mm, (Figs. 2 and 4)
D_{CCD}	*Miscanthus* stem diameter observed on the Charge Coupled Device (CCD), pixel, (Fig. 4)
D_{TRUE}	True (manually measured) diameter of *Miscanthus* stem, mm, (Fig. 4)
F	Distance from the CCD to the pinhole, pixel (constant, Figs. 2 and 4)
x	Vertical location of Illuminated Line Segment observed on the CCD, pixel, (Fig. 2)
y	Distance projected onto the MxG stem from the Illuminated Line Segment to the upper field of view limit of the camera, mm, (Fig. 2)
y_1	Component of y, mm, (Fig. 2)
y_2	Component of y, mm, (Fig. 2)

this crop grows in clumps and singulating stems would be a time consuming practice. As an alternative, a machine vision-based diameter sensor was developed that employs monocular vision, which lowers the system costs whilst avoiding stereo vision imperatives such as disparity image processing. However, in the absence of stereo vision, to measure diameters in world coordinates, the distance from the camera to the object of interest must be obtained by alternative means. To accomplish this, Teoh and Zhang (1984) acquired stereo images using a single camera in combination with a movable mirror. Nishimoto and Shirai (1987) avoided using mirrors by placing a glass plate in front of the camera that was rotated to provide two independent images. A similar method was also used by Pachidis and Lygouras (2007). Matsumoto, Terasaki, Sugimoto, and Arakawa (1997) used image sequencing from a moving camera to obtain independent images. Criminisi, Reid, and Zisserman (2000) reported on a monocular prior knowledge based vision system, where the depth information was obtained by referencing to an object with a known height in the imagery. Wang and Ishii (2009) developed a system to reconstruct depth information based on optical flow analysis, where a speed sensor was used to determine the acceleration.

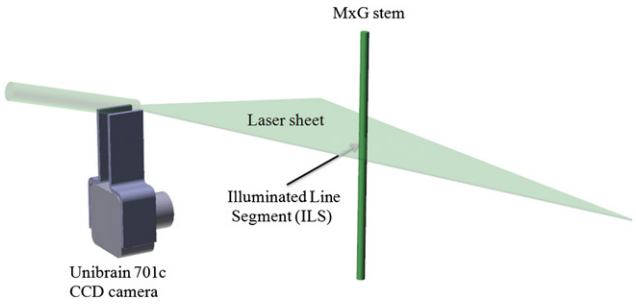

Fig. 1 – Diameter sensing arrangement, featuring a UniBrain® 701c CCD camera fitted with a 6 mm wide angle lens (Pentax® C60607KP). To reduce ambient light disturbance, the camera was fitted with an inline optical filter with a 532 nm centre wavelength, and 10 nm bandwidth (Edmund Scientific, NT65-700). The laser sheet was generated by mounting a Fresnel lens to a 50 mW, 532 nm (green) laser pointer, yielding an aperture angle of 60°. It was slanted downward at an angle of 15°, yielding a detectable depth range from approximately 350–1500 mm. The camera detected the Illuminated Line Segment projected onto a *Miscanthus* stem, which was used to measure the depth and the stem diameter.

The machine vision system described here employs structured lighting in the form of a laser sheet that creates an Illuminated Line Segment (ILS) on any reflecting object, which can then be detected by a camera. The laser sheet has a constant yaw angle with respect to the camera, allowing determination of the depth from the camera to the ILS whilst circumventing the need for stereo imaging: The geometry dictates that ILSs that are detected at a high vertical pixel location in an image are close to the camera and *vice versa*. In addition, by changing the roll angle of the whole camera/laser sheet arrangement, the orientation of the ILS can be varied, allowing the dimensions of objects along arbitrary planes to be measured. A more complicated situation emerges when the method would be applied as a phenotyping tool in crops such as maize, where organs protruding from the stem such as crown roots, leaves, ears, and tassels complicate the measurements. This problem is exacerbated when using the method to phenotype intricate structures such as roots. Arguably, the easiest target of the slanted laser sheet method in agriculture would be a stand of harvest-ready MxG stems. This is mainly because the stand in late winter or early spring resembles a set of tall stems since the leaves fall off during autumn. Therefore, the problem can be abstracted as comprising a set of tall, vertical, convex, cylindrical, reflecting objects that are randomly anchored in a target area.

The method as described could be used in the development of a Look Ahead Yield Monitor (LAYM) for MxG: knowing the average biomass per area would be a component of the Precision Agriculture paradigm, but in addition, it could be used to control the speed of a harvester, allowing the machine to operate at maximum throughput capacity, whilst optimizing its field capacity. The LAYM concept consists of determining the material volume of the stand, yielding the biomass per target area through multiplication by the true material density in kg m^{-3}. The volume of the stand in the target area could be determined by 1) measuring the average stem diameter, 2) counting the number of stems, and 3) measuring the average crop height. The method as described here only enables 1) and 2). Item 3) will be addressed in a separate manuscript by the authors. Counting the number of stems in itself is not trivial, since an estimate of the number of occluded stems needs to be determined based on

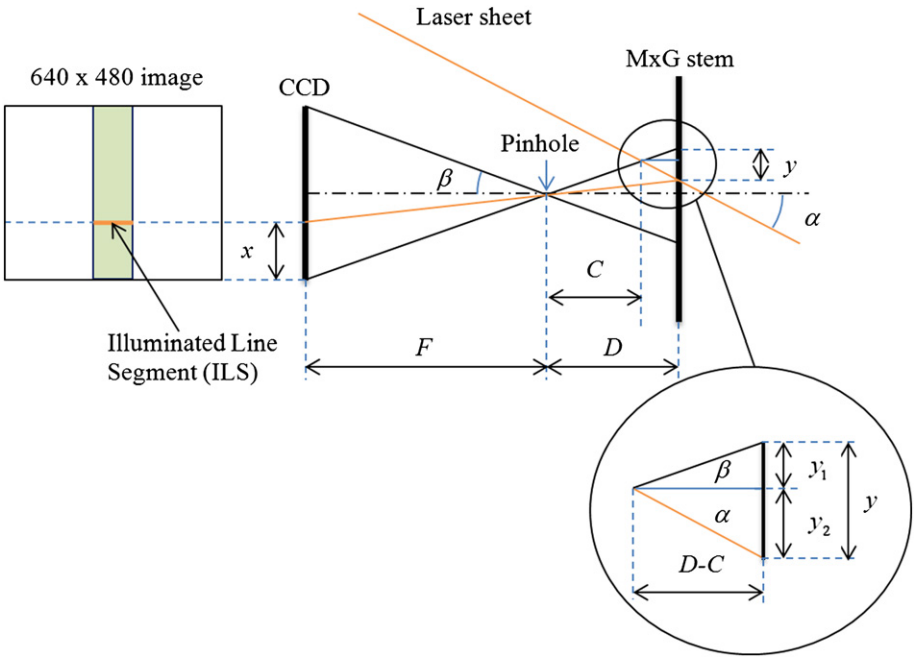

Fig. 2 – Lateral view camera pinhole model used to determine the relationship between the distance between the pinhole and the stem ("depth") *D* in mm, and the observed height of the Illuminated Line Segment *x* in pixels, as observed in the image shown on the left.

the observed number of visible ones. The same occlusion issue arises in the diameter measurement problem. The method as shown here can determine the stem that is closest to the camera (and not partially occluded) by detecting the highest ILS in the image, but there is no guarantee that other stems are not partially occluded. The system in its present form is unable to determine automatically whether an ILS is partially occluded, but this feature may be added in the future: The problems of counting stems, in addition to determining mean stem diameters, are similar to research reported by Grift and Crespi (2008a,b). They used coverage process theory, assuming a Poisson arrival distribution, to estimate the number of particles and the mean particle diameter in a granular flow regime. Although the hypothesis of a Poisson process driving the locations of MxG stems is untested here, these papers may serve as a starting point for future statistical modelling of counting/diameter measurement under occlusion.

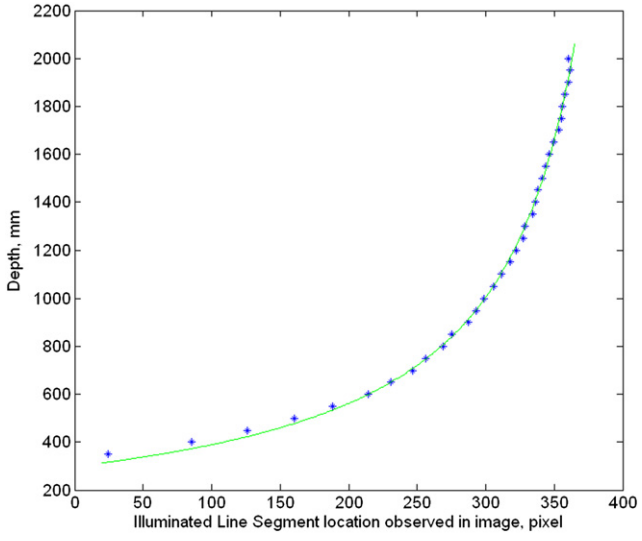

Fig. 3 – Measured relationship between the depth *D* in mm, and the observed Illuminated Line Segment location *x* in pixels, as observed in the image as shown in Fig. 2 on the left. A theoretical curve derived from the geometric analysis based on Fig. 2 was fitted, leading to a coefficient of determination of 0.998.

The objective of this research was to 1) develop a generic, reliable, field-ready diameter sensor for stalk type crops, and 2) to evaluate its performance under field conditions using MxG stems as test objects.

2. Materials and methods

The measurement principle, as illustrated in Fig. 1, is comprised of a CCD camera (Unibrain® Fire-i 701c) that observes an ILS, projected onto an MxG stem by a laser sheet. Since the downward slope angle of the laser sheet is constant (15°), the distance from the camera to the MxG stem can be determined using the vertical location of the observed line segment on the CCD. The known distance also enables measurement of the MxG stem diameter, since the relationship between world and camera coordinates is known through camera calibration.

The laser sheet was created by mounting a Fresnel lens on a 50 mW, 532 nm (green) laser diode. This resulted in a laser

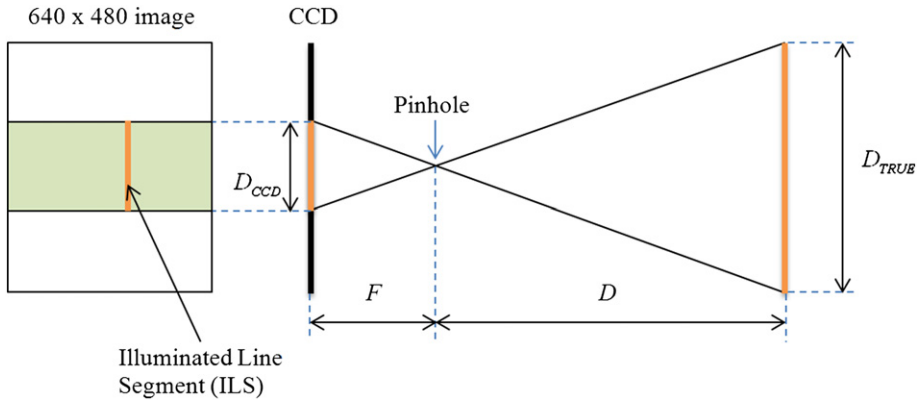

Fig. 4 – Top view camera pinhole model used to calibrate the *Miscanthus* stem diameter measurement. The aim was to determine the relationship between the true stem diameter (right) and the corresponding width of the Illuminated Line Segment in pixels in the image shown on the left, assuming that the depth *D* in mm is known from a separate measurement. *F* is a constant camera parameter in pixel.

sheet with an approximate thickness of 2 mm and an aperture angle of 60°. The camera was fitted with a variable focus/variable aperture, C-mount lens with a focal length of 6 mm (Pentax, C60607KP). To reduce ambient light disturbance, the camera was fitted with an inline optical filter with a 532 nm centre wavelength, and 10 nm bandwidth (Edmund Scientific, NT65-700). A portable computer was used to control the camera through a 1394 FireWire® interface and acquire images with a resolution of 640 × 480 pixels. The camera was calibrated using a standard procedure contained in a MatLab® toolbox based on Tsai's method (Tsai, 1987), which enabled distortion correction of the imagery.

2.1. *Geometrical analysis for depth and diameter estimation*

Fig. 2 shows a lateral view pinhole camera model combined with a downward slanted laser sheet. On the right, the target (MxG stem) is shown. The camera contains a Charge Coupled Device (CCD) chip which consists of 480 pixels in the vertical direction. The image, as shown on the left, observes a part of the MxG stem, which contains the line segment that is illuminated by the laser sheet (ILS). The challenge is now to determine how the distance between the pinhole and the MxG stem ("depth", *D*) in mm affects the observed ILS height (x, in pixels) in the image. Employing similarity of triangles, the following relationships were derived:

$$\left.\begin{aligned} y &= y_1 + y_2 \\ \tan\alpha &= \frac{y_2}{D-C} \\ \tan\beta &= \frac{y_1}{D-C} \end{aligned}\right\} y = (D-C)(\tan\alpha + \tan\beta) \quad (1)$$

where *D* is the "depth" (distance from the camera pinhole to the object) in mm, α represents the downward slope of the laser sheet in °, and the angle β in ° was determined by calibration of the camera using chessboard images, a procedure stated by Zhang (1999). *C* in mm is the distance between the pinhole and the intercept between the upper field of view limit of the camera and the laser sheet. *F* in pixel is the constant distance from the CCD to the camera pinhole. In addition, the geometry dictates that:

$$\frac{x}{F} = \frac{y}{D} \quad (2)$$

Combining Eq. (1) and Eq. (2) yields:

$$D = \frac{CF(\tan\alpha + \tan\beta)}{F(\tan\alpha + \tan\beta) - x} \quad (3)$$

where *C*, *F*, α, β are constants once the camera and laser sheet are fixed in position. The values of *F* and *C* were determined using calibration where the sensing system was moved so as

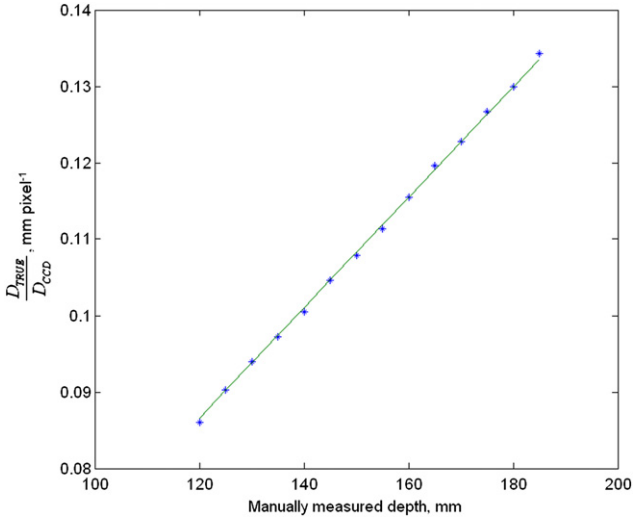

Fig. 5 – Calibration result allowing the calibration of the camera parameter F. A chessboard image was acquired at varying, manually measured, depths and the ratio between a true constant distance consisting of multiple chessboard squares and the corresponding distance on the CCD in pixels was determined for each depth. The slope of the line in the figure is equal to the reciprocal value of F.

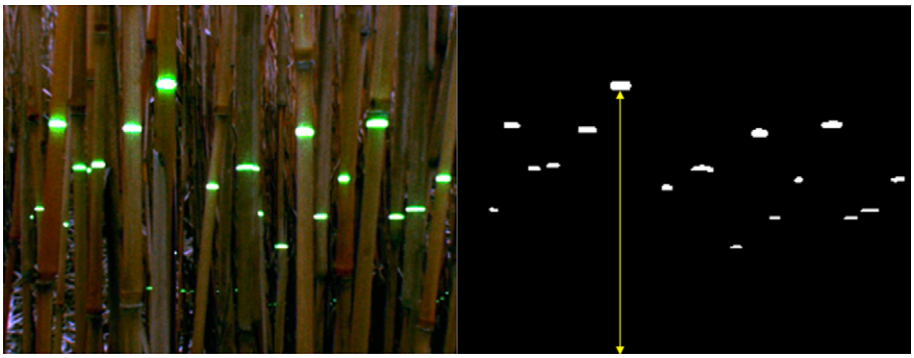

Fig. 6 – Left: Image of MxG stems with laser intercepts. Notice that some of the Illuminated Line Segments (ILSs) shown in the image are partially occluded by other stems. These ILSs were excluded from the datasets through threshold filtering. Right: Image as shown on the left, after segmentation and removal of partially occluded ILSs. The arrow indicates the observed height of the Illuminated Line Segment on the CCD in pixel (variable *x* in Fig. 2).

to project the laser sheet at depths ranging from 350 mm to 2000 mm at 50 mm intervals on a flat ground surface, whilst recording the observed vertical distances (in pixels) in the images. Subsequently, Eq. (3) was fitted on the dataset (Fig. 3), which resulted in the following relationship with a coefficient of determination of 0.998:

$$D = \frac{127200}{426.6 - x} \tag{4}$$

The second relationship needed to measure the diameter of stems translated the width of the laser sheet interceptions on the stems observed in an image in pixels to a diameter in mm. Fig. 4 shows a top view of the pinhole camera model with the CCD on the left side consisting of 640 horizontal pixels. Similarity of triangles gives:

$$\frac{D_{TRUE}}{D_{CCD}} = \frac{1}{F}D \tag{5}$$

where D_{TRUE} in mm is the true diameter of the MxG stem at the location of the ILS, D in mm is the depth obtained from Eq. (4), and D_{CCD} in pixel is the MxG stem diameter observed on the CCD. To calibrate the constant $1/F$, a chessboard was placed at depths (D) ranging from 120 to 190 mm in increments of 5 mm, and the number of pixels representing a fixed number of squares on the chessboard was recorded allowing calculation of the ratio D_{TRUE}/D_{CCD} in mm pixel^{-1} (Fig. 5). The value of $1/F$ is now equal to the slope of the linear fit line in Fig. 5 being $7.2 \cdot 10^{-4}$ pixel^{-1} with a coefficient of determination of 0.999. To calculate the diameter of the MxG stems, Eq. (5) was solved for D_{TRUE}, using D_{CCD}, the observed MxG diameter on the CCD in pixels, as well as the measured depth D as inputs.

2.2. *Target identification and diameter measurement*

Before processing the images, automatic white balancing was applied following a method developed by Weng, Chen, and Fuh (2005). Fig. 6 (left) shows an example image where the laser sheet is intercepted by multiple MxG stems. Owing to the downward inclination of the laser sheet, ILSs that are higher in the image are closer to the camera and *vice versa*. The colour image was thresholded and converted to a binary image. Rudimentary filtering of partially occluded ILSs was accomplished by selecting only those ILSs representing stems larger than the smallest stem diameter encountered during experiments (3.1 mm). The depth from the camera pinhole to a stalk was calculated from the distance in pixels from the top of the image to an ILS (as indicated by the arrow in Fig. 6(right)). This value was entered as the variable x in Eq. (4) to obtain the depth to this ILS. Subsequently, the MxG stalk diameter was calculated by substituting the width of the intercept in pixels, along with the depth D in mm from Eq. (4), into Eq. (5).

3. Results

To evaluate the performance of the developed diameter sensor, it was tested in an MxG field in Urbana, Illinois (lat, lon: 40.042686, −88.237871), during the autumn of 2010 and spring

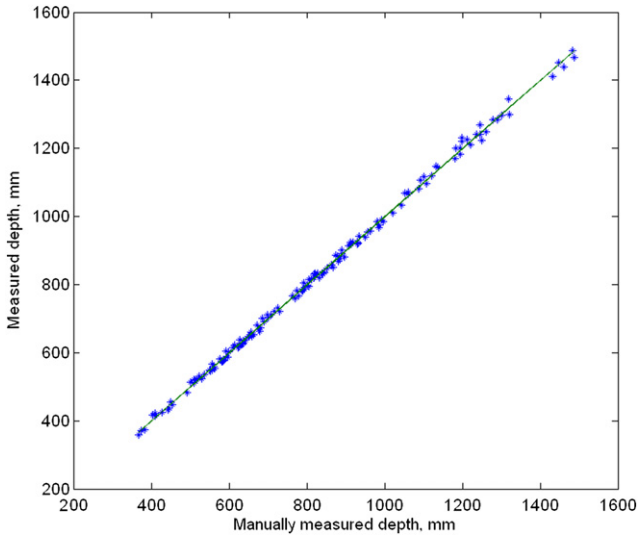

Fig. 7 – Measured depths from the camera to *Miscanthus* stems in mm, versus corresponding manually measured depths in mm yielding a slope of 1.002, an intercept of −1.2 mm and a coefficient of determination of 0.998.

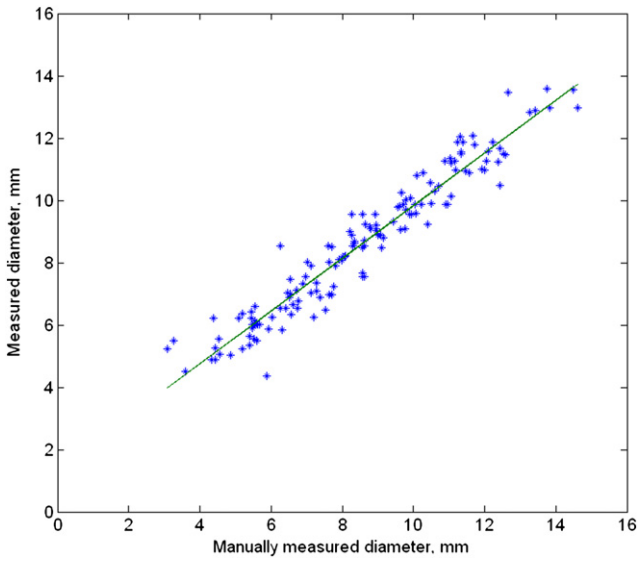

Fig. 8 – Measured diameters of *Miscanthus* stems in mm, versus corresponding manually measured diameters in mm, yielding a slope of 0.845, an intercept of 1.4 mm and a coefficient of determination of 0.926.

of 2011 when no leaves were present. The experiments were conducted under varying weather and ambient light conditions at randomly chosen locations in the field. The sensing arrangement was mounted on a tripod, which was levelled to provide a horizontal laser sheet orientation. Among 100 randomly selected images, 1364 MxG stem diameters were measured and among these, 150 MxG stems were manually measured using an electronic calliper. To ensure a fair comparison, the diameters were measured manually while and where the laser sheet projected an ILS onto the stems.

The measured depths, ranging from 368 to 1486 mm, are plotted versus the manually measured depths in Fig. 7. A straight line was fitted, yielding a slope of 1.002, an intercept of −1.2 mm and a coefficient of determination of 0.998.

In addition, the measured diameters, ranging from 3.1 to 14.6 mm are plotted versus the corresponding manually measured diameters in mm, as shown in Fig. 8. A straight line was fitted, yielding a slope of 0.845, an intercept of 1.4 mm and a coefficient of determination of 0.926.

4. Conclusions

A machine vision system was developed that allows measurement of multiple *M. giganteus* (MxG) stem diameters in a single image. The method consisted of projecting an Illuminated Line Segment (ILS) onto the MxG stem, which was detected by a CCD camera. The vertical location of the ILS on the CCD allowed for the determination of the distance between camera and the MxG stalk (depth): Subsequently, the MxG stem diameter was measured by evaluating the width of the ILS on the CCD.

The measurement arrangement proved adequate in terms of detection of ILSs under field and varying light conditions. The depth measurements ranging from 368 to 1486 mm in the field were compared to their manually measured counterparts, yielding a straight line relationship with a slope of 1.002, an intercept of −1.2 mm and a coefficient of determination of 0.998.

The stem diameter measurements, ranging from 3.1 to 14.6 mm, were also compared with manual calliper-based measurements. Here another straight line relationship was found, yielding a slope of 0.845, an intercept of 1.4 mm and a coefficient of determination of 0.926.

An important limitation of the method, inherent in evaluating multiple stems in a single image simultaneously, was partial occlusion of stems by other stems. In this research ILSs were removed from the datasets, by filtering based on a known smallest stem diameter. In the future an automated algorithm needs to be developed to automatically determine occlusion, without prior knowledge of the stem diameter distribution.

REFERENCES

Clifton-Brown, J. C., Breuer, J., & Jones, M. B. (2007). Carbon mitigation by the energy crop, *Miscanthus*. *Global Change Biology, 13*(11), 2296–2307. doi:10.1111/j.1365-2486.2007.01438.x.

Clifton-Brown, J. C., & Lewandowski, I. (2002). Screening *Miscanthus* genotypes in field trials to optimise biomass yield and quality in southern Germany. *European Journal of Agronomy, 16*(2), 97–110.

Criminisi, A., Reid, I., & Zisserman, A. (2000). Single view metrology. *International Journal of Computer Vision, 40*(2), 123–148. doi:10.1023/A:1026598000963.

Delwiche, M., & Vorhees, J. (2003). Optoelectronic system for counting and sizing field-grown deciduous trees. *Transactions of the ASAE, 46*(3), 877–882.

Grift, T. E., & Crespi, C. (2008a). Estimating mean particle diameter in free-fall granular particle flow using a Poisson model in space. *Biosystems Engineering, 101*, 28–35. doi:10.1016/j.biosystemseng.2008.06.005.

Grift, T. E., & Crespi, C. (2008b). Estimation of the flow rate of free falling granular particles using a Poisson model in time. *Biosystems Engineering, 101*, 36–41. doi:10.1016/j.biosystemseng.2008.06.006.

Grift, T. E., & Oberti, R. (2006). Development of low-cost root collar diameter measurement devices for pine seedlings. *Computers and Electronics in Agriculture, 52*, 60–70. doi:10.1016/j.compag.2006.01.005.

Heaton, E. A., Clifton-Brown, J. C., Voigt, T. B., Jones, M. B., & Long, S. P. (2004). *Miscanthus giganteus* for renewable energy generation: European Union experience and projections for Illinois. *Mitigation and Adaptation Strategies for Global Change, 9*(4), 433–451. doi:10.1023/B:MITI.0000038848.94134.be.

Lewandowski, I., Scurlock, J. M., Lindvall, E., & Christou, M. (2003). The development and current status of perennial rhizomatous grasses as energy crops in the US and Europe. *Biomass and Bioenergy, 25*(4), 335–361. doi:10.1016/S0961-9534(03)00030-8.

Matsumoto, Y., Terasaki, H., Sugimoto, K., & Arakawa, T. (1997). A portable three-dimensional digitizer. In *Proceedings of the international conference on recent advances in 3-D digital imaging and modeling* (pp. 197–204).

McDonald, T. P., Rummer, R. B., & Grift, T. E. (2003). Diameter sensors for tree-length harvesting systems. In M. I. Wide, & B. Baryd (Eds.), *2nd forest engineering conference* (pp. 45–54), Vaxjo, Sweden.

Michel, R., Rapagna, S., Di Marcello, M., Burg, P., Matt, M., Courson, C., et al. (2011). Catalytic steam gasification of *Miscanthus x giganteus* in fluidised bed reactor on olivine based catalysts. *Fuel Processing Technology, 92*(6), 1169–1177. doi:10.1016/j.fuproc.2010.12.005.

Nishimoto, Y., & Shirai, Y. (1987). A feature-based stereo model using small disparities. *Proceedings Computer Vision and Pattern Recognition*, 192–196.

Pachidis, T. P., & Lygouras, J. N. (2007). Pseudostereo-vision system: a monocular stereo-vision system as a sensor for real-time robot applications. *IEEE Transactions on Instrumentation and Measurement, 56*(6), 2547–2560. doi:10.1109/TIM.2007.908231.

Teoh, W., & Zhang, X. (1984). An inexpensive stereoscopic vision system for robots. *IEEE Proceedings International Conference on Robotics and Automation*, 186–189. doi:10.1109/ROBOT.1984.1087176.

Tsai. (1987). A versatile camera calibration technique for high-accuracy 3D machine vision metrology using off-the-shelf TV cameras and lenses. *IEEE Journal of Robotics and Automation, 3*(4), 323–344. doi:10.1109/JRA.1987.1087109.

Wang, X., & Ishii, K. (2009). Depth perception using a monocular vision system. In M. K. al (Ed.), *ICONIP 2008, part I, LNCS. 5506* (pp. 779–786). Springer-Verlag. doi:10.1007/978-3-642-02490-0_95.

Weng, C. C., Chen, H., & Fuh, C. S. (2005). A novel automatic white balance method for digital still cameras. *IEEE International Symposium on Circuits and Systems, 4*, 3801–3804. doi:10.1109/ISCAS.2005.1465458.

Yamamoto, H., Yamaji, K., & Fujino, J. (1999). Evaluation of bioenergy resources with a global land use and energy model formulated with SD technique. *Applied Energy, 63*(2), 101–113. doi:10.1016/S0306-2619(99)00020-3.

Zhang, Z. (1999). Flexible camera calibration by viewing a plane from unknown orientations. *Proceedings of the Seventh IEEE International Conference on Computer Vision, 1*, 666–673. doi:10.1109/ICCV.1999.791289.

Zub, H. W., Arnoult, S., & Brancourt-Hulmel, M. (2011). Key traits for biomass production identified in different *Miscanthus* species at two harvest dates. *Biomass and Bioenergy, 35*(1), 637–651. doi:10.1016/j.biombioe.2010.10.020.